Quantum theory of amplified total internal reflection due to evanescent-mode coupling

Chang-Woo Lee,[1] Kyungbum Kim,[1] Jaewoo Noh,[2] and Wonho Jhe[1,*]
[1]*Center for Nearfield Atom-Photon Technology and Physics Department, Seoul National University, Seoul 151-742, Korea*
[2]*Physics Department, Inha University, Inchon 402-751, Korea*
(Received 3 March 2000; published 13 October 2000)

We present a quantum theory of the amplification of light undergoing a total internal reflection. We show that the light amplification is due to the stimulated emission of evanescent-mode photon from the active region of the interface. Our theoretical results are in good agreement with experimental observations and provide deeper understanding of the quantum-mechanical characteristics of the evanescent wave. A corresponding triplet-mode laser theory is also presented.

PACS number(s): 42.50.Ct, 42.55.−f, 03.70.+k

I. INTRODUCTION

Light amplification by indirect coupling to an active medium through an evanescent wave has been used as a new lasing method, in particular in waveguide optics [1–9]. It has been observed experimentally that when the light wave propagating in a passive dielectric medium is totally reflected at the planar interface between the dielectric and a pumped active medium, the reflectance can be greater than unity. This means that the amplification of light is possible even though the light beam propagates only in the passive medium [10–12]. There have been several previous attempts to explain this enhanced internal reflection (EIR) [11,13–15]. Many authors have commonly introduced a complex refractive index having a negative imaginary part for the active medium to explain the phenomenon. A similar approach was also used to describe the amplification process in a waveguide having an active-cladding region [16,17].

However, these classical theories using macroscopic constants are rather phenomenological, and even provide a wide range of values for the optical gain. Therefore, an exact and full quantum theory is needed to understand the EIR process at a microscopic and fundamental level. There has been only speculation that the EIR may be possibly due to the stimulated emission of photons from the active region where the evanescent wave is present. One difficulty in understanding the EIR phenomena is related to the question of how the photon emitted by the stimulated process follows the direction of the reflected wave instead of that of the incident wave. A simple model of incident plane wave having a definite momentum vector and the subsequent tunneling of the incident photon into the active medium is not enough to give a satisfactory answer. We intend to show that it is possible to explain the EIR phenomenona by using a quantized triplet mode [18], using a proper form of the Hamiltonian for the atom–evanescent-field interaction.

In this paper, we present a full quantum-mechanical description of light amplification by the stimulated emission of the evanescent-mode photon in the EIR process. In particular, we show that the cavity QED effect, which is absent in the classical theory, plays an important role in the correct description of the EIR or the evanescent-field amplifier (EFA) in general. We also present a lasing theory that includes the evanescent wave coupled to the atomic system, which has not been treated in the usual text books, and calculate the optical gain for two sample systems. Our theory offers a deeper understanding of the photon concept in the atom–evanescent-field interaction.

II. TRIPLET-MODE QUANTIZATION

In 1971, Carniglia and Mandel presented a quantization theory of the electromagnetic waves including the evanescent wave throughout all the region with a half space filled with a homogeneous dielectric medium [18]. They considered a space filled with a passive medium having a uniform refractive index n to the left of the plane $z=0$ $(z<0)$, and the empty space to the right of the plane $(z>0)$. Triplet modes consisting of incident, reflected, and transmitted waves were introduced and it was shown that the triplet modes form a set of orthogonal modes. The triplet modes are classified by the left (L) and right (R) modes depending on the incident-wave directions, and by the polarizations [transverse electric (TE) and transverse magnetic (TM) components].

Carniglia *et al.* [19] then verified experimentally the validity of the triplet-mode theory by performing a measurement of light absorption and emission mediated by the evanescent wave. Here we present only a brief summary of their results needed to develop our theory. First, the refractive index function $n(\mathbf{r})$ is given by

$$n(\mathbf{r})=\begin{cases} n & \text{for } z<0 \\ 1 & \text{for } z>0. \end{cases} \tag{1}$$

We denote by $\mathbf{k}$ and $\mathbf{K}$, respectively, the wave vector in the left-hand (dielectric) and right-hand (vacuum) half space with their components given by

$$k_1=K_1, \quad k_2=K_2, \quad k=nK, \tag{2}$$

$$k_3=\pm\sqrt{(nK)^2-k_1^2-k_2^2}, \tag{3}$$

$$K_3=\pm\sqrt{K^2-K_1^2-K_2^2}. \tag{4}$$

*Corresponding author. Email address: whjhe@snu.ac.kr

 ©2000 The American Physical Society

In particular, for incident waves from the left-hand space, we have

$$k_3 = nK\cos\theta, \tag{5}$$

$$K_3 = K\sqrt{1-n^2\sin^2\theta}, \tag{6}$$

where θ is the angle of incidence. Consequently, K_3 is imaginary as the angle of incidence exceeds the critical angle $\theta_c = \sin^{-1}(1/n)$, so that the triplet mode contains the evanescent wave in that case.

The electric field operator in the triplet-mode representation is then obtained as

$$\hat{\mathbf{E}} = \sum_{\mathbf{k}}\sum_{s}\sqrt{\frac{2\pi\hbar\omega_{\mathbf{k}}}{V}}[\hat{a}_{L,\mathbf{k},s}\mathbf{E}_{L,\mathbf{k},s}(\mathbf{r})e^{-i\omega_{\mathbf{k}}t} + \text{H.c.}] + \sum_{\mathbf{K}}\sum_{s}\sqrt{\frac{2\pi\hbar\omega_{\mathbf{K}}}{V}}[\hat{a}_{R,\mathbf{K},s}\mathbf{E}_{R,\mathbf{K},s}(\mathbf{r})e^{-i\omega_{\mathbf{K}}t} + \text{H.c.}]. \tag{7}$$

Here $\omega_{\mathbf{k}} = c|\mathbf{k}|/n, \omega_{\mathbf{k}} = c|\mathbf{K}|$, and s denotes the polarization direction (TE or TM mode). $\hat{a}_{L,\mathbf{k},s}$ and $\hat{a}_{R,\mathbf{K},s}$ are the annihilation operators of the left-hand and right-right mode, respectively. The explicit forms of the mode functions $\mathbf{E}_{L,\mathbf{k},s}$, etc. are given in Appendix A, and the relevant orthogonality relation is obtained by integrating over all the space with the weight function $n^2(\mathbf{r})$ as

$$\frac{1}{V}\int \mathbf{E}^*_{A,\mathbf{k},s}(\mathbf{r})\cdot\mathbf{E}_{A',\mathbf{k}',s'}(\mathbf{r})n^2(\mathbf{r})d^3r = \delta_{AA'}\delta_{\mathbf{k}\mathbf{k}'}\delta_{ss'}, \tag{8}$$

where A and A' stand for the L and R modes.

III. SPONTANEOUS DECAY RATE

Since the triplet modes form a set of orthogonal modes that already include the effect of media given by the Fresnel relations, a single triplet mode can be treated as an effective free electromagnetic-field mode. In the sense that a photon is an excitation of the quantized electromagnetic field, and that the triplet mode already includes the effect of the boundary in the quantization process, the triplet-mode photon should be considered to interact with the atom in the same way as the conventional plane-wave photon. The interaction of the atom with the triplet-mode photon is then treated as a small perturbation. Considering the usual interaction Hamiltonian in the dipole approximation

$$H_I = -\mathbf{d}\cdot\mathbf{E}, \tag{9}$$

which shows that the interaction is related to the atomic dipole moment and the electromagnetic field amplitude at the location of the atom, one can carry out the calculation for the atomic transition rates by using the triplet-mode electromagnetic field.

The calculation of the spontaneous-emission transition rate is then straightforward by applying Fermi's golden rule,

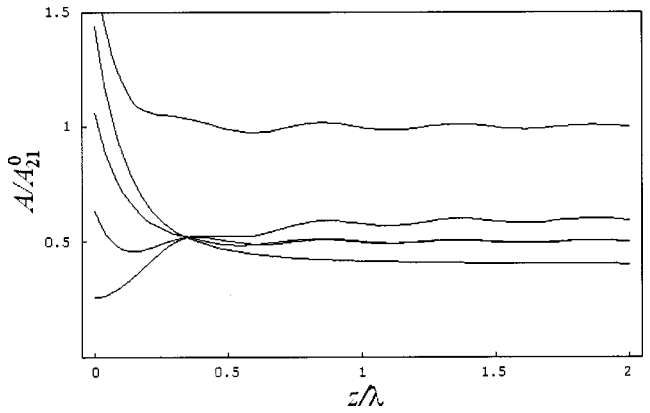

FIG. 1. Decay rates according to the L and R modes for the dielectric with refractive index $n=1.5$. Note that $A_{21} > A_L > A_{\text{TM}} > A_{\text{TE}} > A_R$ at $z=0$.

$$A_{21} = \frac{2\pi}{\hbar}\sum_{\alpha}|\langle 1|H_I|2\rangle|^2\delta(\hbar\omega_\alpha - \hbar\omega_0). \tag{10}$$

Here $\hbar\omega_0 = E_2 - E_1$ is the transition energy between the level $|2\rangle$ and $|1\rangle$ of an atom, and α stands for the triplet-mode index. We use the notation A_{21} in connection with Einstein's theory for the forthcoming discussions. If the atom is at $\mathbf{r}=(x,y,z)$ in the space $R(z>0)$, the matrix element $\langle 1|H_I|2\rangle$ is proportional to

$$\begin{aligned} &-\int_{z'>0}\psi_1^*(\mathbf{r}'-\mathbf{r})[\mathbf{E}_\alpha(\mathbf{r}')\cdot\mathbf{d}]\psi_2(\mathbf{r}'-\mathbf{r})d^3\mathbf{r}' \\ &= -\mathbf{E}_\alpha(\mathbf{r})\cdot\int_{z'>-z}\psi_1^*(\mathbf{r}')\mathbf{d}\psi_2(\mathbf{r}')d^3\mathbf{r}' \\ &= -\mathbf{E}_\alpha(\mathbf{r})\cdot\langle 1|\mathbf{d}|2\rangle, \end{aligned} \tag{11}$$

where we have used the dipole approximation, and extended the integration range into the whole space, since the atomic wave function is well localized in the half space.

Consequently, the transition rate can be written as

$$A_{21} = \frac{(2\pi)^2}{\hbar V}\sum_{\alpha}\omega_\alpha|\mathbf{E}_\alpha\cdot\mathbf{d}_{12}|^2\delta(\omega_\alpha - \omega_0), \tag{12}$$

where $\mathbf{d}_{12} = \langle 1|\mathbf{d}|2\rangle$. For convenience, we will use $\mathbf{d} = \mathbf{d}_\parallel + \mathbf{d}_\perp = \mathbf{d}_\parallel + d_3\hat{z}$ instead of $\mathbf{d}_{12}$ hereafter. As an illustration, we can obtain alternative representations of A_{21} by splitting the decay rate according to the L and R, TE, and TM, $\mathbf{d}_\parallel$ and $\mathbf{d}_\perp$ modes, as

$$A_{21} = \frac{2}{3}A^\parallel + \frac{1}{3}A^\perp, \tag{13}$$

$$= A_{\text{TE}} + A_{\text{TM}}, \tag{14}$$

$$= A_L + A_R, \tag{15}$$

where the detailed functional forms of the above quantities are derived in Appendix B, and the functional dependences on the atom-boundary separation are presented Fig. 1. Note

that, from the above expressions, one can see the various contributions to the modified decay rate, which are important in calculating the radiation pattern due to spontaneous emission.

We find that as n increases, the emission rate into the left-hand mode decreases. Moreover, when $n\rightarrow\infty$, A_L approaches zero, whereas A_R reduces to that of a perfect conductor [20–22]. It is this cavity-QED effect [22,23] that has been overlooked by previous classical descriptions (this is not negligible, in particular, for a thin active medium). Similar results of the spontaneous emission rate were obtained by other authors [24] using a different formalism, and our theoretical results are in good agreement with them. We want to point out that there is a difference between the spontaneous emission rate of the L mode and R mode in their dependence on the atom location, as shown in Fig. 1. This can be understood as being due to the fact that when we deal with the spontaneous emission into the triplet modes as classified by the incident wave, the L mode and R mode are distinguished because of the causality. We can also find the interference effect in the emission rate of the R mode.

IV. EVANESCENT-MODE GAIN AND LASER THEORY

Let us begin with the basic steps of the first-principles laser theory described in [25]. Since the direction of the reflected wave is predetermined in the triplet mode, the direction of the stimulated emission is also determined accordingly. Therefore, we only have to calculate the strength of the atom-photon interaction in the triplet-mode representation, as in the ordinary case of no interface. This is an advantage of employing the triplet mode for the description of the amplification process due to the stimulated emission of the evanescent-mode photon. Now we first calculate the induced absorption rate using Fermi's golden rule for a given evanescent mode $\alpha=(\mathbf{k},\mathrm{TE})$,

$$\Gamma_{1\rightarrow 2}=B_{21}\left|\frac{2k_3e^{iK_3z}}{n(k_3+K_3)}\right|^2\frac{n_\alpha\hbar\omega_\alpha}{V}\delta(\omega_\alpha-\omega_0). \tag{16}$$

Here $B_{21}=4\pi^2|\mathbf{d}_{12}|^2/3\hbar^2$ is the ordinary Einstein B coefficient in free space and we obviously assume $iK_3<0$ and the nondegeneracy of levels. Note that the A and B coefficients are not simply related as in the thermal equilibrium case, since we are dealing with the nonisotropic distribution of radiative energy density.

Moreover, if we consider broadband light, we may approximate

$$\frac{n_\alpha\hbar\omega_\alpha}{V}\delta(\omega_\alpha-\omega_0)\rightarrow\int dw_\alpha W_0(\omega_\alpha)\delta(\omega_\alpha-\omega_0), \tag{17}$$

where $W_0(\omega)d\omega$ is the ordinary incident beam energy density in the range $[\omega,\omega+d\omega]$. For the description of the interaction of atom and triplet-mode photon, we now define

$$W(\omega_\alpha,\mathbf{r})=n^2(\mathbf{r})|\mathbf{E}_\alpha(\mathbf{r})|^2W_0(\omega_\alpha), \tag{18}$$

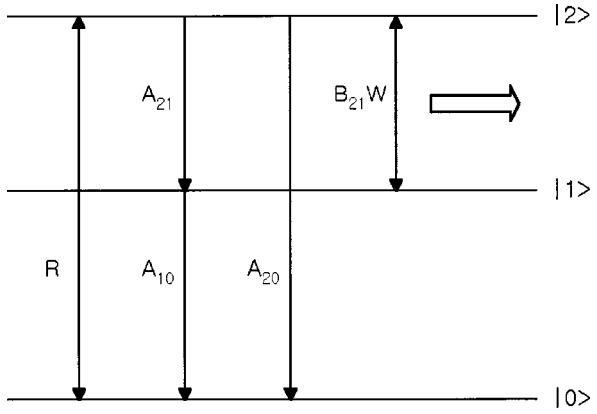

FIG. 2. Three-level lasing system. Lasing occurs between $|2\rangle$ and $|1\rangle$, and $|0\rangle$ is the ground state. Each letter denotes the appropriate transition rate.

as the real spectral energy density in the triplet-mode representation. Then the corresponding transition rate can be written as

$$\Gamma_{1\rightarrow 2}=B_{21}W(\omega_\alpha,\mathbf{r}), \tag{19}$$

in a similar way to the usual case. Note that the rate is proportional to the mode function $|\mathbf{E}_\alpha(\mathbf{r})|^2$, which was confirmed by the absorption experiment of Carniglia *et al.* [19].

We also find that the total electromagnetic energy in the triplet-mode description is equivalent to the sum of total photon energies, as in the ordinary case:

$$\frac{1}{V}\int d^3\mathbf{r}\int d\omega_\alpha W(\omega_\alpha,\mathbf{r})=\int d\omega_\alpha W_0(\omega_\alpha)=\frac{1}{V}\sum_\alpha n_\alpha\hbar\omega_\alpha, \tag{20}$$

where we have used Eq. (8). Consequently, we can reach the conclusion that although there are definite n photons per single mode, the atom experiences different energy density due to the factor $|\mathbf{E}_\alpha(\mathbf{r})|^2$, and hence the atom exhibits different transition rates depending on its position. Based on the calculations of A_{21} and $\Gamma_{1\rightarrow 2}$, the general stimulated-emission transition rate in the presence of dielectric interface can be calculated in a similar way, using the triplet mode-approach.

Now, if we assume that the atom placed above the dielectric is a simple three-level system (Fig. 2), we obtain the following steady-state value of the population inversion:

$$N_2-N_1=\frac{R(A_{10}-A_{21})}{A_{10}(A_{20}+A_{21})+B_{21}W(A_{10}+A_{20})}, \tag{21}$$

where N_i is the ith level's population density such that $N_1+N_2+N_3=1$, R is the pumping rate, and A_{ij} is the decay rate from $|i\rangle$ to $|j\rangle$. Assuming that the reflected beam is a plane wave in the far zone, one can obtain the amplified energy per unit of time, which will be added to the reflected beam, resulting from the stimulated emission by the excited atoms at $\mathbf{r}$ above the dielectric as

$$(N_2-N_1)F(\omega)d\omega B_{21}W(\omega,\mathbf{r})\hbar\omega\rho_A(\mathbf{r})d^3r = \delta I_{\mathrm{incr}}d\omega S\cos\theta, \tag{22}$$

where $F(\omega)$ is the line-shape function of the atom and ρ_A is the atomic density. Here δI_{incr} is the increased spectral intensity of the reflected beam and S is the area of the interface between the dielectric medium and the active medium (S is infinite in the case of the plane wave, but it will be eliminated later).

Finally, an expression for the gain is obtained as

$$I_\alpha/I_\alpha^0 = 1+\int_{z>0} G_\alpha\ dz, \tag{23}$$

where $I_\alpha^0(I_\alpha)$ is the incident (reflected) beam intensity for a single-mode field and

$$G_\alpha = \frac{R(A_{10}-A_{21})}{A_{10}(A_{20}+A_{21})}\frac{\rho_A(\mathbf{r})B_{21}\hbar\omega_\alpha F(\omega_\alpha)}{c\cos\theta} \times\frac{|\mathbf{E}_\alpha(\mathbf{r})|^2}{1+(I_0/I_s)|\mathbf{E}_\alpha(\mathbf{r})|^2}. \tag{24}$$

Here we have used $I_\alpha^0 = cW_0(\omega_\alpha)/n$ and defined the saturation intensity as

$$I_s = \frac{A_{10}(A_{20}+A_{21})}{(A_{10}+A_{20})}\frac{c}{nB_{21}}. \tag{25}$$

Since the gain medium is not in the propagating region of the light wave, the integration in Eq. (23) is not performed over the propagation distance of the wave but over the active medium's depth. Thus the gain formula does not have the usual exponential form even for the case where the incident beam has sufficiently low intensity. Moreover, even if the incident beam (intensity I_α^0) is strong enough to saturate the gain medium in the ordinary case, the evanescent-wave characteristics of exponential decay ($|\mathbf{E}_\alpha(\mathbf{r})|^2$) indicates that the penetrated beam is not strong far from the boundary, so that the gain G_α shows a different saturation behavior with respect to the ordinary laser. It is these facts that make the difference between this and the usual lasing theory. Note that the single-mode gain is explicitly given in Eq. (23) in terms of the microscopic properties of an active medium. The same formula can be applied to the atomic gas, or a single impurity atom in a dielectric solid, and the amount of gain will depend strongly on the location of the atom. Note also that it is the square of the evanescent field that determines the amount of gain, so that a connection to the semiclassical theory can be established.

V. SAMPLE CALCULATION

With the practical assumption that $A_{20}\approx 0$, $A_{21}\ll A_{10}$, the gain coefficient formula given in Eq. (24) simply becomes, neglecting the saturation effect,

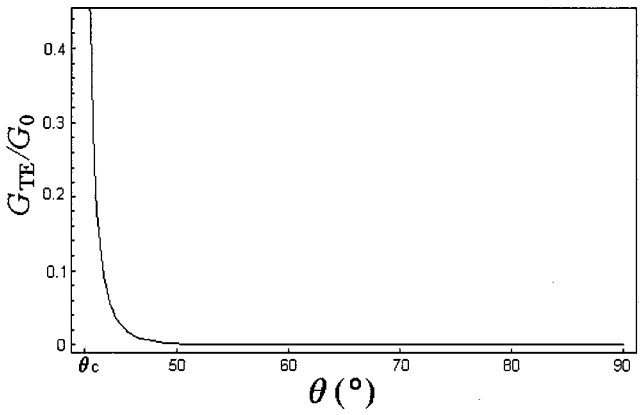

FIG. 3. He-Ne gas gain coefficient for TE mode with respect to the incident angle at $z=\lambda$.

$$G_\alpha = G_0\frac{A_{21}^0}{A_{21}}\frac{|\mathbf{E}_\alpha(\mathbf{r})|^2}{\cos\theta}, \tag{26}$$

where G_0 is the ordinary unsaturated gain coefficient of a laser system. This approximate expression is obtained in the three-level system, but it can be also applied to more general systems as long as the spontaneous-decay rate of the main laser transition is much smaller than the others. Note that, in principle, the value of G_0 can be calculated from Eq. (24) if the experiment details, such as the pumping rate, are known.

In explaining the experimental results of the pulsed (broadband) laser by Kogan *et al.* [10] where the active medium was rhodamine-6G mixed with nitrobenzene in ethyl-alcohol, Callary and Carniglia [14] used a complex amplitude reflectance whose absolute value is greater than one, and could estimate a gain coefficient of $\gamma=0.000\,15$, which was obtained by taking into account the known emission cross section of the dye, the molar concentration, and the thickness of the active medium $d=250\lambda$ in the experiment. This gain coefficient γ, which includes the experiment details, is related to the ordinary laser-gain coefficient G_0 by $G_0=4\pi\gamma/\lambda$. Accordingly, we find $G_0=4.7\times10^3\mathrm{m}^{-1}$ for the experiment of [10] and consequently we obtain the gain >25, which agrees well with the phenomenological theory as well as the experimental result.

Let us consider another example where a laser beam with a narrow linewidth is used and the active medium above the dielectric is a Doppler-broadened He-Ne gas, assuming that it is an effective three-level system. For a typical He-Ne laser tube, $G_0=0.15\,\mathrm{m}^{-1}$ [26] and therefore we can estimate the optical gain when the active medium is a typical gas laser system. Since the optical gain for a gas laser is small, in general the evanescent wave gain is also calculated to be as small as about 0.0001.

In Fig. 3, we have plotted the He-Ne gain coefficient [Eq. (26)] for the TE mode with respect to the incident angle at $z=\lambda$. As can be observed, the gain coefficient reaches its peak value near the critical angle of the internal reflection (refer also to Fig. 4). In Fig. 4, the He-Ne gain coefficients versus z at several incident angles are also presented. Note that the atom-location dependence of the gain changes rapidly as the incident angle approaches the critical angle. The

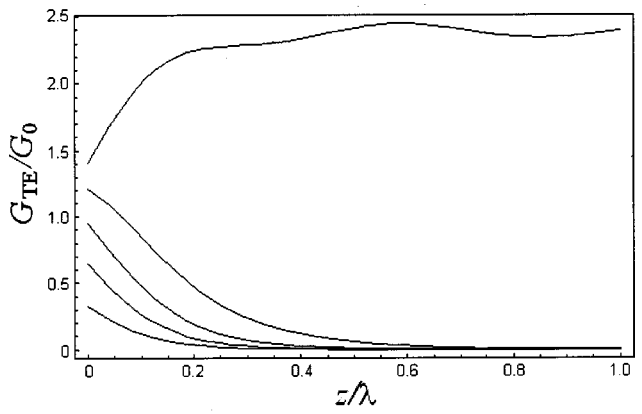

FIG. 4. He-Ne gain coefficients for TE mode versus z at incident angles of $\theta=80°$, $70°$, $60°$, $50°$, θ_c from the bottom. Note that the gain coefficient at $\theta=\theta_c$ becomes smallest at $z=0$ due to the largest decay rate at the boundary.

reason the gain due to the atom near the interface is reduced when the light incidence angle is close to the critical angle is that the spontaneous decay rate is increased as the atom moves closer to the boundary. This quantum effect is difficult to find in the classical theory.

VI. CONCLUSION

We have derived the spontaneous-emission and the stimulated-emission transition rates for an atom near a dielectric medium using the quantized triplet modes of the electromagnetic field. To the best of our kowledge, it is the first time that a full quantum theory of stimulated emission from an atom coupled to the evanescent field has been established. The nature of the stimulated emission of an evanescent-mode photon is characterized with the help of the quantized triplet-mode concept. Although the spontaneous-decay rate can also be calculated using the linear response theory [22], we have obtained a simple expression for the decay rate showing explicitly the dependence of the decay rate on the atomic dipole moment, the location of the atom, and the emission direction.

The quantum-mechanically-derived induced-transition rate, showing a functional behavior similar to that of the classical theory, provides clearer and more direct insights supported by the quantum-optical viewpoint. We also have shown that the quantum effect shows up when the atom is located close to the interface, which affects the amplification gain significantly.

Moreover, using the transition rates, which depend sensitively on specific parameters such as the active medium's thickness, atomic dipole moments, atom density, and the incident angle of the light, we have formulated a laser theory for the propagating light coupled to the nonpropagation region. This amplification concept is common to all EFA systems, hence our model may also be applied to, especially, waveguide optics.

ACKNOWLEDGMENT

This work was supported by the Creative Research Initiatives of the Korean Ministry of Science and Technology.

APPENDIX A: TRIPLET-MODE WAVE FUNCTIONS

The classical mode functions are given only in the right-hand space ($z>0$) needed for our theory and we have rewritten those into more convenient forms as

$$\mathbf{E}_{L,\mathbf{k},\mathrm{TE}}(\mathbf{r})=\mathbf{E}^{(T)}_{L,\mathbf{k},\mathrm{TE}}(\mathbf{r})=\hat{\varepsilon}\frac{1}{n}\frac{2k_3}{k_3+K_3}e^{i\mathbf{K}\cdot\mathbf{r}}$$
$$=(\hat{K}_\parallel\times\hat{z})\frac{1}{n}\frac{2k_3}{k_3+K_3}e^{i\mathbf{K}\cdot\mathbf{r}}, \tag{A1}$$

$$\mathbf{E}_{L,\mathbf{k},\mathrm{TM}}(\mathbf{r})=\mathbf{E}^{(T)}_{L,\mathbf{k},\mathrm{TM}}(\mathbf{r})=(\hat{\varepsilon}\times\hat{K})\frac{2k_3}{k_3+n^2K_3}e^{i\mathbf{K}\cdot\mathbf{r}}$$
$$=\left(\frac{K_\parallel}{K}\hat{z}-\frac{K_3}{K}\widehat{K_\parallel}\right)\frac{2k_3}{k_3+n^2K_3}e^{i\mathbf{K}\cdot\mathbf{r}}, \tag{A2}$$

$$\mathbf{E}_{R,\mathbf{K},\mathrm{TE}}(\mathbf{r})=\mathbf{E}^{(I)}_{R,\mathbf{K},\mathrm{TE}}(\mathbf{r})+\mathbf{E}^{(R)}_{R,\mathbf{K},\mathrm{TE}}(\mathbf{r})$$
$$=\hat{\varepsilon}e^{i\mathbf{K}\cdot\mathbf{r}}+\hat{\varepsilon}\frac{K_3-k_3}{K_3+k_3}e^{i\mathbf{K}^R\cdot\mathbf{r}}$$
$$=2\frac{\hat{K}_\parallel\times\hat{z}}{K_3+k_3}[K_3\cos K_3z+ik_3\sin K_3z]e^{i\mathbf{K}_\parallel\cdot\mathbf{r}}, \tag{A3}$$

$$\mathbf{E}_{R,\mathbf{K},\mathrm{TM}}(\mathbf{r})=\mathbf{E}^{(I)}_{R,\mathbf{K},\mathrm{TM}}(\mathbf{r})+\mathbf{E}^{(R)}_{R,\mathbf{K},\mathrm{TM}}(\mathbf{r})$$
$$=(\hat{\varepsilon}\times\hat{K})e^{i\mathbf{K}\cdot\mathbf{r}}+(\hat{\varepsilon}\times\hat{K}^R)\frac{n^2K_3-k_3}{n^2K_3+k_3}e^{i\mathbf{K}^R\cdot\mathbf{r}}$$
$$=\frac{2}{K(n^2K_3+k_3)}\{K_\parallel\hat{z}[n^2K_3\cos K_3z+ik_3\sin K_3z]$$
$$-K_3\hat{K}_\parallel[k_3\cos K_3z+in^2K_3\sin K_3z]\}e^{i\mathbf{K}_\parallel\cdot\mathbf{r}}, \tag{A4}$$

where I,R,T denote incident, and reflected, and transmitted waves, $\mathbf{K}_\parallel$ is the parallel component of $\mathbf{K}=\mathbf{K}_\parallel+K_3\hat{z}$, $\mathbf{K}^R=\mathbf{K}_\parallel-K_3\hat{z}$ is the reflectedwave vector of $\mathbf{K}$, and $\hat{K}_\parallel$ is a unit vector in the direction of $\mathbf{K}_\parallel$.

APPENDIX B: VARIOUS DECAY RATES

For real calculations of the decay rates, we convert summations into integrations using

$$\sum_{\mathbf{k}}\rightarrow\frac{V}{(2\pi)^3}\int d^3\mathbf{K},\quad \sum_{\mathbf{k}}\rightarrow\frac{V}{(2\pi)^3}\int d^3\mathbf{k} \tag{B1}$$

and we obtain

$$A^{\parallel}_{L,\mathrm{TE}}=\frac{K_0|\mathbf{d}_{\parallel}|^2}{4\pi\hbar}\int_{k_3>0}d^3\mathbf{k}\,\delta(k/n-K_0)\left|\frac{2k_3e^{iK_3z}}{n(k_3+K_3)}\right|^2, \tag{B2}$$

$$A^{\perp}_{L,\mathrm{TE}}=0, \tag{B3}$$

$$A^{\parallel}_{L,\mathrm{TM}}=\frac{K_0|\mathbf{d}_{\parallel}|^2}{4\pi\hbar}\int_{k_3>0}d^3\mathbf{k}\,\delta(k/n-K_0)\left|\frac{K_3}{K}\,\frac{2k_3e^{iK_3z}}{k_3+n^2K_3}\right|^2, \tag{B4}$$

$$A^{\perp}_{L,\mathrm{TM}}=\frac{K_0|\mathbf{d}_{\perp}|^2}{2\pi\hbar}\int_{k_3>0}d^3\mathbf{k}\,\delta(k/n-K_0)\left|\frac{K_{\parallel}}{K}\,\frac{2k_3e^{iK_3z}}{k_3+n^2K_3}\right|^2, \tag{B5}$$

$$A^{\parallel}_{R,\mathrm{TE}}=\frac{K_0|\mathbf{d}_{\parallel}|^2}{4\pi\hbar}\int_{K_3<0}d^3\mathbf{K}\,\delta(K-K_0)\times\left|2\frac{K_3\cos K_3z+ik_3\sin K_3z}{K_3+k_3}\right|^2, \tag{B6}$$

$$A^{\perp}_{R,\mathrm{TE}}=0, \tag{B7}$$

$$A^{\parallel}_{R,\mathrm{TM}}=\frac{K_0|\mathbf{d}_{\parallel}|^2}{4\pi\hbar}\int_{K_3<0}d^3\mathbf{K}\,\delta(K-K_0)\times\left|2\frac{K_3}{K}\,\frac{k_3\cos K_3z+in^2K_3\sin K_3z}{n^2K_3+k_3}\right|^2, \tag{B8}$$

$$A^{\perp}_{R,\mathrm{TM}}=\frac{K_0|\mathbf{d}_{\perp}|^2}{2\pi\hbar}\int_{K_3<0}d^3\mathbf{K}\,\delta(K-K_0)\times\left|2\frac{K_{\parallel}}{K}\,\frac{n^2K_3\cos K_3z+ik_3\sin K_3z}{n^2K_3+k_3}\right|^2, \tag{B9}$$

where $K_0=\omega_0/c$.

Now we define the decay rates according to the left-hand and right-hand modes, TE and TM, $\mathbf{d}_{\parallel}$ and $\mathbf{d}_{\perp}$

$$A^{\parallel}=A^{\parallel}_{L,\mathrm{TE}}+A^{\parallel}_{L,\mathrm{TM}}+A^{\parallel}_{R,\mathrm{TE}}+A^{\parallel}_{R,\mathrm{TM}}, \tag{B10}$$

$$A^{\perp}=A^{\perp}_{L,\mathrm{TE}}+A^{\perp}_{L,\mathrm{TM}}+A^{\perp}_{R,\mathrm{TE}}+A^{\perp}_{R,\mathrm{TM}}, \tag{B11}$$

$$A_{\mathrm{TE}}=\frac{2}{3}A^{\parallel}_{L,\mathrm{TE}}+\frac{1}{3}A^{\perp}_{L,\mathrm{TE}}+\frac{2}{3}A^{\parallel}_{R,\mathrm{TE}}+\frac{1}{3}A^{\perp}_{R,\mathrm{TE}}, \tag{B12}$$

$$A_{\mathrm{TM}}=\frac{2}{3}A^{\parallel}_{L,\mathrm{TM}}+\frac{1}{3}A^{\perp}_{L,\mathrm{TM}}+\frac{2}{3}A^{\parallel}_{R,\mathrm{TM}}+\frac{1}{3}A^{\perp}_{R,\mathrm{TM}}, \tag{B13}$$

$$A_L=\frac{2}{3}A^{\parallel}_{L,\mathrm{TE}}+\frac{1}{3}A^{\perp}_{L,\mathrm{TE}}+\frac{2}{3}A^{\parallel}_{L,\mathrm{TM}}+\frac{1}{3}A^{\perp}_{L,\mathrm{TM}}, \tag{B14}$$

$$A_R=\frac{2}{3}A^{\parallel}_{R,\mathrm{TE}}+\frac{1}{3}A^{\perp}_{R,\mathrm{TE}}+\frac{2}{3}A^{\parallel}_{R,\mathrm{TM}}+\frac{1}{3}A^{\perp}_{R,\mathrm{TM}}, \tag{B15}$$

where 2/3 and 1/3 comes from the orientational average with both $\mathbf{d}_{\parallel}$ and $\mathbf{d}_{\perp}$ replaced by $\mathbf{d}$.

Also when $n\rightarrow 1$, the decay rate reduces to the free-space one, i.e.,

$$\begin{aligned}A_{21}&=\frac{2}{3}A^{\parallel}_{L,\mathrm{TE}}+\frac{1}{3}A^{\perp}_{L,\mathrm{TE}}+\frac{2}{3}A^{\parallel}_{L,\mathrm{TM}}+\frac{1}{3}A^{\perp}_{L,\mathrm{TM}}+\frac{2}{3}A^{\parallel}_{R,\mathrm{TE}}\\&\quad+\frac{1}{3}A^{\perp}_{R,\mathrm{TE}}+\frac{2}{3}A^{\parallel}_{R,\mathrm{TM}}+\frac{1}{3}A^{\perp}_{R,\mathrm{TM}}\rightarrow\frac{1}{4}A^0_{21}+0+\frac{1}{12}A^0_{21}\\&\quad+\frac{1}{6}A^0_{21}+\frac{1}{4}A^0_{21}+0+\frac{1}{12}A^0_{21}+\frac{1}{6}A^0_{21}\\&=A^0_{21}\end{aligned} \tag{B16}$$

where $A^0_{21}=4K_0^3|\mathbf{d}_{12}|^2/3\hbar$ is the ordinary free-space spontaneous emission rate.

[1] C.J. Koester, IEEE J. Quantum Electron. **QE-2**, 580 (1966).
[2] K. Sasaki, T. Fukao, T. Saito, and O. Hamano, J. Appl. Phys. **51**, 3090 (1980).
[3] H. Injeyan, O.M. Stafsudd, and N.G. Alexopoulos, Appl. Opt. **21**, 1928 (1982).
[4] N. Periasamy, Appl. Opt. **21**, 2693 (1982).
[5] B.F. Lamouroux, A.G. Orszag, B.S. Prade, and J.Y. Vinet, Opt. Lett. **8**, 504 (1983).
[6] W.V. Sorin, K.P. Jackson, and H.J. Shaw, Electron. Lett. **19**, 820 (1983).
[7] William Y. Liu and Oscar M. Stafsudd, Appl. Opt. **29**, 3114 (1990).
[8] V.A. Kozlov, A.S. Svakhin, and V.V. Ter-Mikirtychev, Electron. Lett. **30**, 42 (1994).
[9] V.A. Kozlov, V.V. Ter-Mikirtychev, and T. Tsuboi, Electron. Lett. **31**, 2104 (1995).
[10] B.Ya. Kogan, V.M. Volkov, and S.A. Lebedev, Pis'ma Zh. Éksp. Teor. Fiz. [JETP Lett. **16**, 100 (1972)].
[11] S.A. Lebedev, V.M. Volkov, and B.Ya. Kogan, Opt. Spectrosc. **35**, 565 (1973).
[12] S.A. Lebedev and B.Ya. Kogan, Opt. Spectrosc. **48**, 564 (1980).
[13] G.N. Romanov and S.S. Shakhidzhanov, Pis'ma Zn. Éksp. Teor. Fiz. **16**, 298 (1972) [JETP Lett. **16**, 209 (1972)].
[14] P.R. Callary and C.K. Carniglia, J. Opt. Soc. Am. **66**, 775 (1976).
[15] R.F. Cybulski, Jr. and C.K. Carniglia, J. Opt. Soc. Am. **67**, 1620 (1977).
[16] K.O. Hill, A. Watanabe, and J.G. Chambers, Appl. Opt. **11**, 1952 (1973).
[17] K.O. Hill, R.I. MacDonald, and A. Watanabe, J. Opt. Soc. Am. **64**, 263 (1974).
[18] C.K. Carniglia and L. Mandel, Phys. Rev. D **3**, 280 (1971).
[19] C.K. Carniglia, L. Mandel and K.H. Drexhage, J. Opt. Soc. Am. **62**, 479 (1972).
[20] E.A. Power and T. Thirunamachandran, Phys. Rev. A **25**, 2473

(1982).
[21] Peter W. Milonni, *The Quantum Vacuum* (Academic Press, San Diego, 1994), Sec. 6.2.
[22] J.M. Wylie and J.E. Sipe, Phys. Rev. A **30**, 1185 (1984); D. Meschede, W. Jhe, and E.A. Hinds, *ibid.* **41**, 1587 (1990).
[23] Maciej Janowicz and Wladyslaw Zakowicz, Phys. Rev. A **50**, 4350 (1994).
[24] J.-Y. Courtois, J.-M. Courty, and J.C. Mertz, Phys. Rev. A **53**, 1862 (1996).
[25] Rodney Loudon, *The Quantum Theory of Light*, 2nd ed. (Oxford University Press, Oxford, 1983), Secs. 5.5 and 1.12.
[26] William T. Silfvast, *Laser Fundamentals* (Cambridge University Press, Cambridge, England, 1996), Sec. 7.6.